Int. J. Electrochem. Sci., 15 **(2020)** 2399 – 2413, doi: 10.20964/2020.03.43

International Journal of ELECTROCHEMICAL SCIENCE
www.electrochemsci.org

Synthesis of Nitrogen and Phosphorus co-doped Carbon with Tunable Hierarchical Porous Structure from Rice Husk for High Performance Supercapacitors

Yuning Qu[1], *Lin Liu*[1], *Lisha Li*[1], *Shuya Wen*[2], *Dan Wei*[2], *Ningru Xiao*[3], *Feng Yan*[1], *Jianguo Yu*[1*], *Lili Wang*[1*]

[1] School of Chemistry and Chemical Engineering, Tiangong University, Tianjin 300387, China
[2] School of Enviromental Science and Engineering, Tiangong University, Tianjin 300387, China
[3] School of Physical Science and Technology, Tiangong University, Tianjin 300387, China
[*]E-mail: wanglili@tjpu.edu.cn; hh_y1118@hotmail.com

Received: 19 October 2019/ *Accepted:* 11 December 2019 / *Published:* 10 February 2020

Nitrogen and phosphorus co-doped porous carbon(N/P-PC) was prepared via a simple direct pyrolysis method using rice husks as the carbon source and H_3PO_4 as the phosphorus source and activator. The acquired products are typical hierarchical porous carbons with a multiple-peaked pore size distribution of microporous and mesoporous structure, which has a high surface area and pore volume. The N_2 adsorption-desorption results show that the mesoporous distribution of N/P-PC can be adjusted in the range of 2-10 nm and the meso-porosity can be varied by changing the H_3PO_4 content. In particular, among the N/P-PC samples, N/P-PC-1:5 has the highest surface area of 2188 m^2/g, pore volume of 3.025 cm^3/g, and pore diameter of 5.537 nm. Electrochemical measurements also indicate that the assembled symmetric cell of N/P-PC-1:5 displays the highest specific capacitance of 236 F/g at a scan rate of 5 mV/s and 130 F/g at a current density of 0.5 A/g; it also has an excellent capacity retention of 100 % after 6000 cycles. The hierarchical porous structure and the synergistic action of nitrogen and phosphorus contribute to the advantageous electrochemical performance of the carbon material. The proposed strategy provides a facile method for preparing porous carbon from biomass waste.

Keywords: Co-doping, Rice husk, Supercapacitor, Tunable porous

1. INTRODUCTION

Electrochemical double layer capacitors (EDLC) are considered to have the most potential for energy storage systems because they have a fast charge/discharge capacity[1-6], longer cycle life, and wide operating temperature. The core of the supercapacitors, electrode materials, and properties of supercapacitors depend mainly on the type of electrode material, especially carbon materials such as activated carbon, carbon nanotubes, graphene, and carbon-derived carbons[7-9]. Although fossil fuel-

based precursors have been prepared via physical activation methods (using steamand CO_2) and chemical activation methods (using H_3PO_4, $ZnCl_2$, and KOH) to prepare EDLC electrode materials[10-12], carbon materials using agricultural wastes such as rice husks, corn stalks, potato waste residue, and bamboo as precursors have received increasing interest because of their sustainability and low cost[13-22].

To adjust the electrical and chemical properties of their surfaces, it is important to tailor their electron donor properties by incorporating heteroatoms into carbon materials[23-26]. The addition of heteroatoms can reduce resistance to charge transfer, improve wetting, and improve capacitance performance. At present, modified carbon materials are been mainly incorporated either via single-or double-doping and used representative heteroatoms such as nitrogen (N)[27], phosphorus (P)[28], sulfur (S), and boron (B)[29].Co-doping can enhance the overall performance of a material because of synergistic action, whereas single heteroatom doping only improves one aspect of the properties. Therefore, increasingly more researchers have been conducting research on multi-heteroatom doping in the last few years. Interestingly, because multi-heteroatom co-doped carbon material can produce a bifunctionalor diatomic synergistic effect, the electrical conductivity of the carbon material is improved and the wettability is enhanced[30,31]. It should be noted that nitrogen-doped carbon materials are heteroatom-doped carbon materials that are used for the most supercapacitor electrode materials. Because P is a N-group element, it displays the same number of valence electrons and chemical properties as N,P-doped carbon materials that are rich in electrons.Thus, P-doped carbon materials are attracting the interest of increasingly more researchers. Furthermore, because the diameter of P is much larger than that of C, P-doping causes local structural distortion of the carbon skeleton, and P protrudes from the structure. Therefore, P-doped carbon materials have more active sites, on one hand, and can also overcome thesteric hindrance effect that is caused by the N-doped carbon material, on the other hand. In addition to EDLC, P possesses a lone pair of electrons, which can induce faradaic reactions and result in an increase of the specific capacitance.Therefore, co-doping P and N into the carbon material enables the synergetic advantages of P and N to be further explored, and thus co-doping P and N leads to enhanced pseudocapacitive properties [32,33]. For example, Wang et al. prepared N/P co-doped microporous carbon via direct carbonization of polyaniline using phosphoric acid as an activator, their prepared co-doped porous carbon had a specific capacitance of 154.4 F/g and outstanding stability[34]. Yan et al. reported that they prepared N/P co-doped porous carbon, the materials they obtained had a specific capacitance of 224.9 F/g [35]. Recently, Jin et al. directly carbonized glucose-containing N and P as the precursor; the obtained P/N co-doped porous carbons sample displayed a specific capacitance of 265 F/g and showed 94% capacitance retention after 5000 cycles[36]. In a word, many methods are emerging to promoting the development of heteroatom co-doped carbon. On one hand, practical and effective heteroatomic doping methods are necessary, and on the other hand, it is still necessary and important to incorporate the appropriate pore structure.

In this work, alkali-treated rice husks(RH) were used as the carbon source and the precursor for preparing carbon materials for supercapacitors. To enhance the properties of carbon electrodes, H_3PO_4 was added to the alkali-treated RH as a phosphorus source and pore modifier. This method promoted the formation of phosphorus covalent bonds and also greatly increased the surface area and pore

volume of the carbon materials. The as-obtained carbon materials were evaluated as supercapacitor electrode materials and displayed excellent energy storage performance in aqueous electrolytes. The proposed strategy provides a convenient method for producing N,P co-doped porous carbons from RH and also has potential applications for adsorption, catalysis, and energy storage.

2. EXPERIMENTAL PART

2.1 Materials

The raw material RH was obtained from a rice mill. All of the chemicals were analytical grade and were used as received without further purification.

2.2 Preparation of N/P-PC

Typically, 3 g of rinsed RH was treated with 2 M NaOH solution and heated to 100 ^{o}C for 4 h. The alkali-treated RH was separated from the liquid via vacuum-assisted filtration, washed with distilled water until the pH was neutral, and dried at 120 ^{o}C overnight[37]. To obtain P-doped porous carbon, the alkali-treated RH and solution of 85 wt.% H_3PO_4 were mixed at a ratio that was in the range of 1:4 - 1:7 (w/v); the mixture was dried at 120^{o}C for 24 h to prepare the impregnated sample. The impregnated sample was later carbonized in a muffle furnace at 500^{o}C for 1 h. The resultant powder was washed several times with hot distilled water and dried at 120^{o}C for 24 h. The prepared P-doped porous carbon was denoted as P-PC-X:Y, where X is the weight of the alkali-treated RH (which was kept constant at 1g) and Y indicates the volume of 85 wt.% H_3PO_4. The mass/volume ratio of the alkali-treated RH to 85 wt.% H_3PO_4 was varied at 1:4, 1:5, 1:6, and 1:7. To further modify the sample with nitrogen, the as-prepared P-PC-1:Y samples under went were further nitridation in a N_2 atmosphere at 800 ^{o}C. The obtained specimens are denoted as N/P- PC-1:4, N/P-PC-1:5, N/P-PC-1:6, and N/P-PC-1:7.

2.3 Characterizations

The morphology and dimensions of the samples were observed with a Hitachi H-800 transmission electron microscope (TEM) at an accelerator voltage of 200 kV. Before TEM characterization, the powders were dispersed in absolute ethanol and ultrasonically treated detected. An X-ray diffractometer(XRD, Japan 2200PC) was used to analyze the crystalline phase of the as-prepared sample using Cu Kα radiation (λ=0.1514178 nm) at a scanning rate of 4° min^{-1} in the 2 theta range from 10° to 70°. An X-ray photoelectron spectrometer with Al Kα radiation (XPS, USA EsCALab MKII) was used to analyze the surface chemical species of the samples. An automatic adsorption instrument (Quantacerome AUTOSORB-1C) was used to analyze the N_2 adsorption-desorption isotherms of the activated carbon to measure the surface area and total pore volumes. The BET equation was used to calculate the surface areas of samples.

Cyclic voltammetry (CV) and galvanostatic charge/discharge were performed in a typical two-electrode test cell with an electrolyte of 6 mol/L KOH. The working electrode (about 10 mg and 1.00 cm^2) was a quadrate from a mixture of activated carbon, polytetrafluoroethylene (PTFE), and acetylene black (8:1:1 weight ratio). The reference and counter electrode were a saturation mercury electrode and Pt electrode, respectively. The working and counter electrodes were sandwiched between two foam nickel current collectors. CV was recorded at a scan rate of 5-2000 mV/s over the potential range from 0 to 1V using an electrochemical workstation (CHI660D), and the electric current densities of the galvanostatic charge/discharge was 0.5, 1, 2, and 3A/g using a battery test system (LAND CT2001A Wuhan LAND, China) at room temperature. The total specific capacitance (Cs) was calculated using Eq.(1) and Eq. (2)[38,39].

$$Cs = \frac{2\int IdV}{m \times \Delta V \times \nu} \quad (1)$$

$$Cs = \frac{2I\Delta t}{m \times \Delta V} \quad (2)$$

In Eq. (1) and Eq. (2), I (A) is the average current, m (g) is the mass of one electrode, V (V) is the applied potential window, and t (s) is the discharge time. Energy densities were calculated using the Eq. (3)

$$E = 0.5Cs \times \Delta V^2 \quad (3)$$

where V is the maximum cell potential after the IR drop has been subtracted.

3. RESULTS AND DISCUSSION

3.1 Composition and pore structure

The N/P-PC samples were designed using a simple low temperature activation and carbonization process. SEM and HR-TEM were used to characterize the morphology of the N/P-PC-1:5 specimen. SEM images (Fig.1a) suggest that the sample N/P-PC-1:5 has a porous structure with pores that piled up and with irregular morphology, and this indicates that N/P-PC-1:5 was not obviously affected by the amount of H_3PO_4. An HR-TEM image of N/P-PC-1:5 (Fig.1b) confirmed that the N/P-PC-1:5 sample formed a porous structure and had a partially ordered graphite structure. Obviously, the irregular morphology, well-developed pores, good mobility liquidity, and localized graphite structure in porous carbon enhanced the electrochemical performance of EDLCs.

High-resolution XPS spectra of C1s, N1s, and P2p for N/P-PC samples were recorded to analyze the chemical contents and valence states of the N,P-doped carbon structures. For C1s (Fig.2a), the N/P-PC-1:5 sample was deconvoluted into four bands: a main peak at 284.6 eV, which is assigned to the graphitic structure (C-C sp^2); a peak at 285.4eV, which is attributed to carbon-carbon single bonds (C-C sp^3) or carbon-phosphorous single bonds(C-P) on the carbon matrix; a peak at 288.4 eV,

which is assigned to carbon-oxygen double bonds (O-C=O)[40]; and a peak at 291.4 eV, which is attributed to the π-π* shake-up satellite peak from sp^2-hybridized carbon atoms.

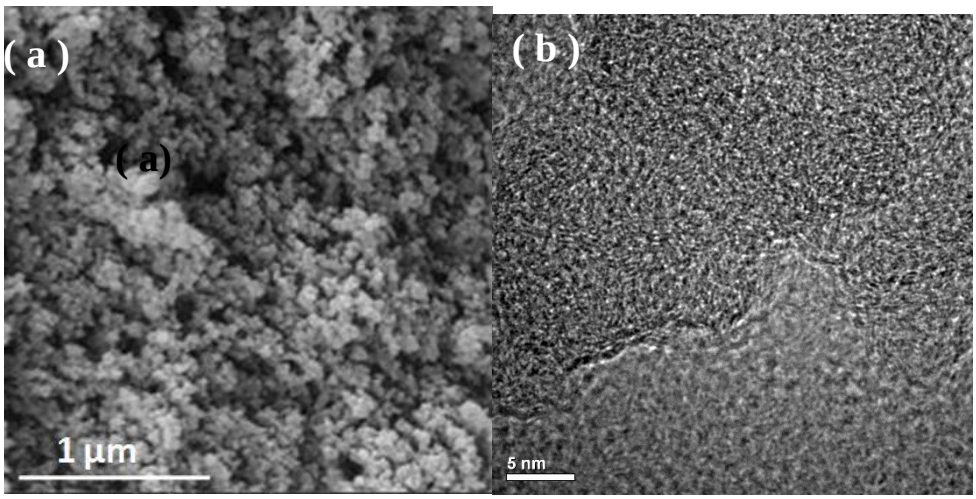

Figure 1. SEM image (a) and HR-TEM image (b) of N/P-PC-1:5.

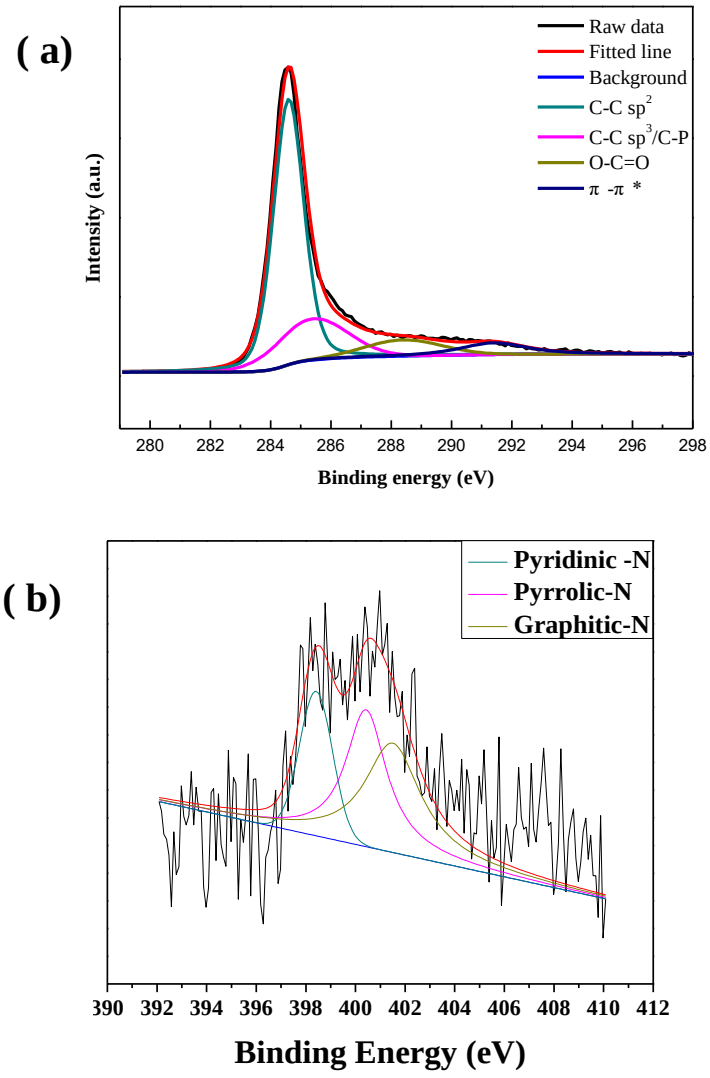

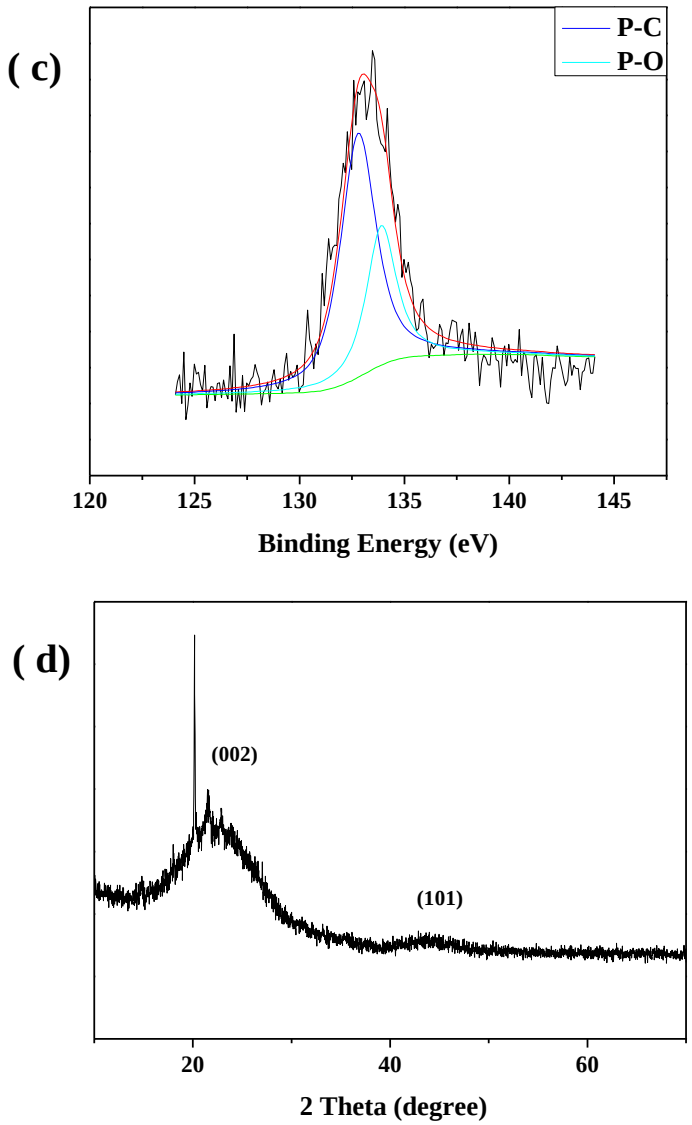

Figure 2. High-resolution XPS spectra of C1s (a), N1s (b), and P2p (c), and XRD pattern of the N/P-PC-1:5 sample (d).

The N1s XPS spectra of the N/P-PC-1:5 sample is shown in Fig 2b. There are three component peaks that indicate the presence of three types of nitrogen functional groups. The peaks at 398.4, 400.4, and 401.4 eV correspond to pyridinic, pyrrolic, and graphitic nitrogen, respectively. The P2p XPS spectra(Fig 2c) for the N/P-PC-1:5 sample exhibited two peaks at 132.8 eV and 133.9 eV, and these are assigned to C-PO_3 and PO_3-O-C bonding, which commonly occur in phosphorus acid-activated carbons, respectively[41]. The presence of P-C bonds confirmed that P was successfully doped in the N/P-PC sample[42]. The crystal structures of the N/P-PC-1:5 materials were measured using wide-angle XRD, as shown in Fig 2d. N and P co-doped carbon materials presented a strong amorphous character, as confirmed by XRD. Two broad peaks at 26° and 43° are observed for N/P-PC-1:5, and these can be easily indexed as the typical (002) and (101) planes of graphitic materials.

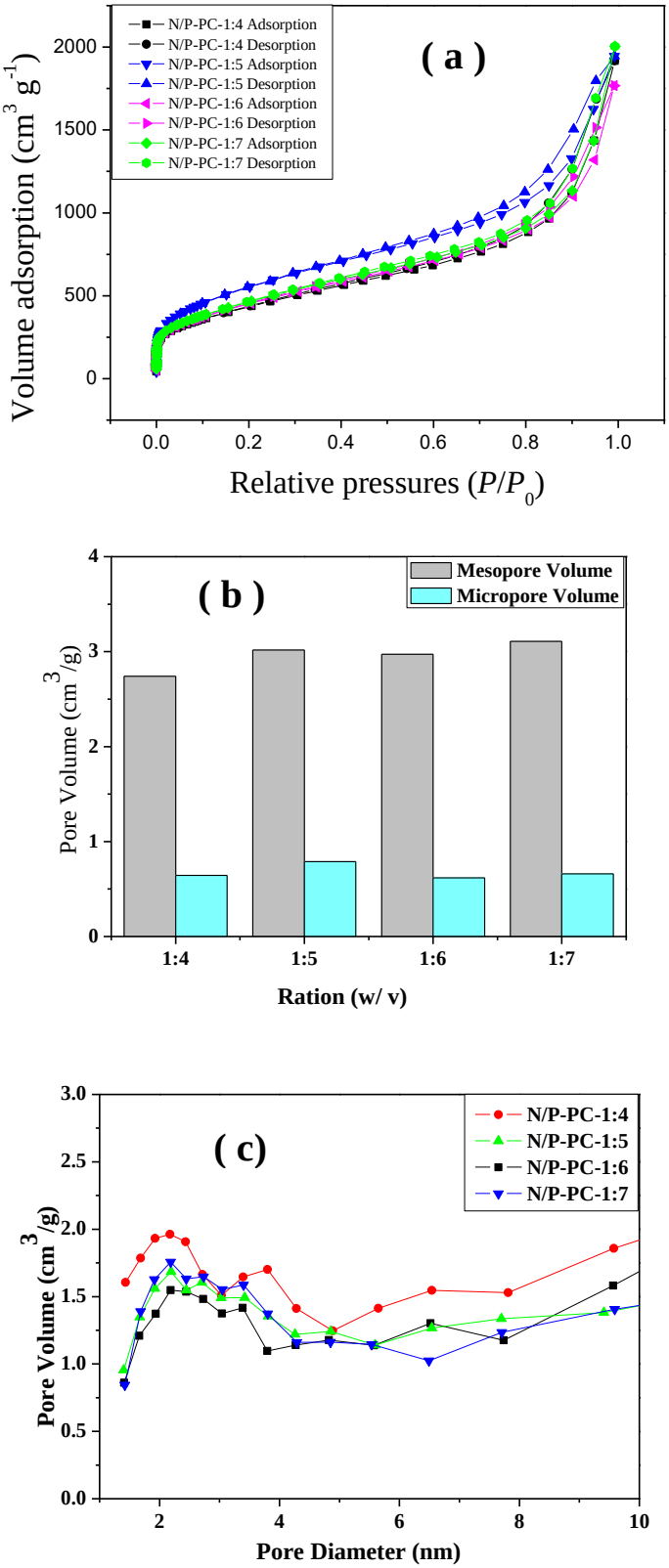

Figure 3. Nitrogen adsorption–desorption isotherms (a), N_2 mesopore volume and micropore volume (b), and pore size distribution (c) of N/P-PC.

To further demonstrate the porous structures of N/P-PC, the surface area, pore volume, and

pore size distribution were determined using nitrogen sorption isotherms. As seen in Fig 3a and 3b, the N/P-PC-1:4, N/P-PC-1:5, N/P-PC-1:6, and N/P-PC-1:7 samples exhibited type IV isotherms with a nearly H4-type hysteresis loop, according to IUPAC classification. It is believed that the H4 hysteresis loop is related to the presence of narrow silty pores that are caused by the piling up of particles[43]. Nitrogen adsorption results are very consistent with the observations from SEM images. Notably, the original porous carbon contains a large number of micropores that cause a hysteresis of divergence at low relative pressure. N_2 adsorption-desorption measurements confirmed the pore characteristics of the N/P-PC sample.

To characterize the pore size distribution curves of the N/P-PC sample, the BJH model and DA method were used to calculate these quantities, respectively. Fig. 3c shows that the pore size distributions of the samples exhibited several peaks. The distribution of micropores and mesopores changed from 1.39 nm to 7.81 nm in N/P-PC-1:5; this observation also confirms that the introduction of N- and P-heteroatoms is an effective way to expand the pore size. Furthermore, co-doping of N and P into the porous carbon matrix increases the mesopore volume. The BET specific surface area of the N/P-PC sample of porous carbon increased from 2063 m^2/g to 2188 m^2/g after N,P co-doping, and this possibly results from pore widening. The N/P-PC samples have a wider pore size distribution and higher mesopore volume, and these factors facilitate rapid ion transfer and improve the high rate performance.

3.2. Electrochemical performance

A series of electrochemical capacitive characteristics of the N/P-PC samples were firstly tested in a two-electrode system. Fig.4a-d shows the CV curves of N/P-PC samples at scan rates from 5 to 2000 mV/s within a voltage window of 0-1 V in 6 M KOH aqueous electrolyte. All of the samples show an approximately rectangular shape with no apparent redox peaks, and this indicates their electrochemical double-layer capacitance characteristics. Obviously, the curve of the N/P-PC-1:5 sample has the best rectangular shape and the largest area, and this indicates that the capacitive behavior of N/P-PC-1:5 is the best. Even at very high scan rates, these rectangular shapes remain good without severe distortion, and thus, they have low equivalent series resistance and an excellent capacitance property. N/P-PC-1:5 is considered to have the largest specific surface area (2188 m^2/g) and an optimal contribution form the nitrogen and phosphorus contents. The specific capacitances calculated form the CV curves at various scan rates for all of the samples are shown in Fig.4e. At a low scan rate of 5 mV/s, N/P-PC-1:5 has a capacitance of 236 F/g, and this gradually decreases to 164 F/g at a scan rate of 500 mV/s and to 146 F/g at a scan rate of 1000 mV/s. The capacitance values of N/P-PC-1:4, N/P-PC-1:6, and N/P-PC-1:7 are 205 F/g, 191 F/g, and 160 F/g, respectively, at 5 mV/s. N/P-PC-1:5 exhibits the largest specific capacitance among all of the N/P-PC samples. However, the capacitance decays greatly with an elevated scan rate.

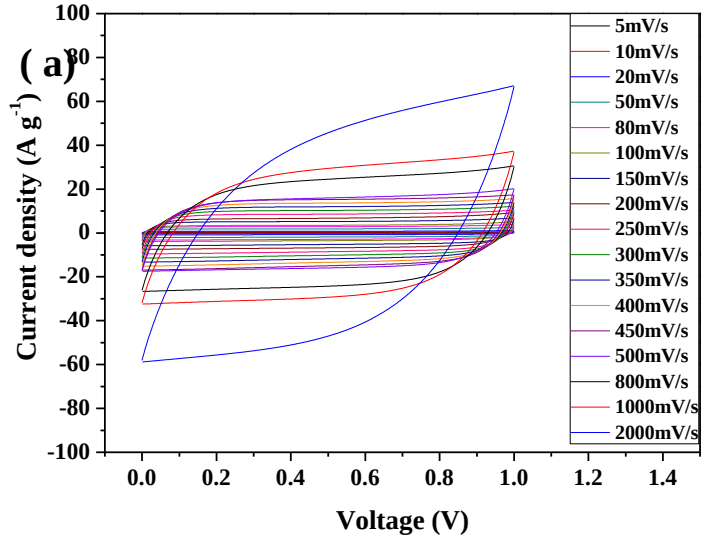
(a)
Current density (A g-1)
Voltage (V)
5mV/s
10mV/s
20mV/s
50mV/s
80mV/s
100mV/s
150mV/s
200mV/s
250mV/s
300mV/s
350mV/s
400mV/s
450mV/s
500mV/s
800mV/s
1000mV/s
2000mV/s

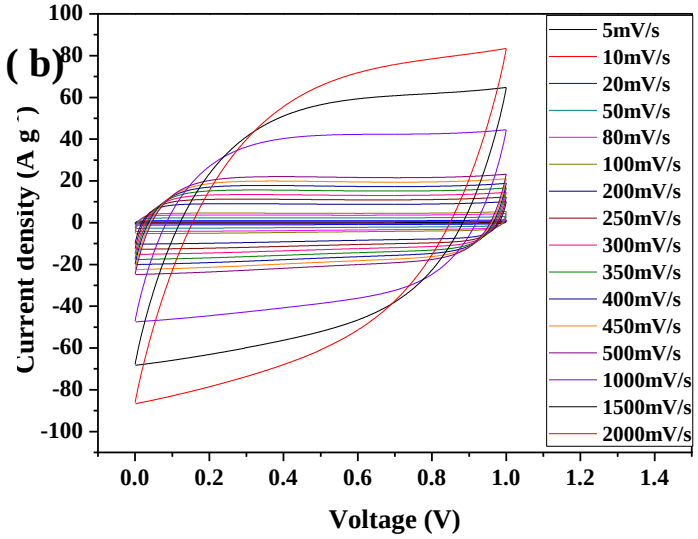
(b)
Current density (A g-1)
Voltage (V)
5mV/s
10mV/s
20mV/s
50mV/s
80mV/s
100mV/s
200mV/s
250mV/s
300mV/s
350mV/s
400mV/s
450mV/s
500mV/s
1000mV/s
1500mV/s
2000mV/s

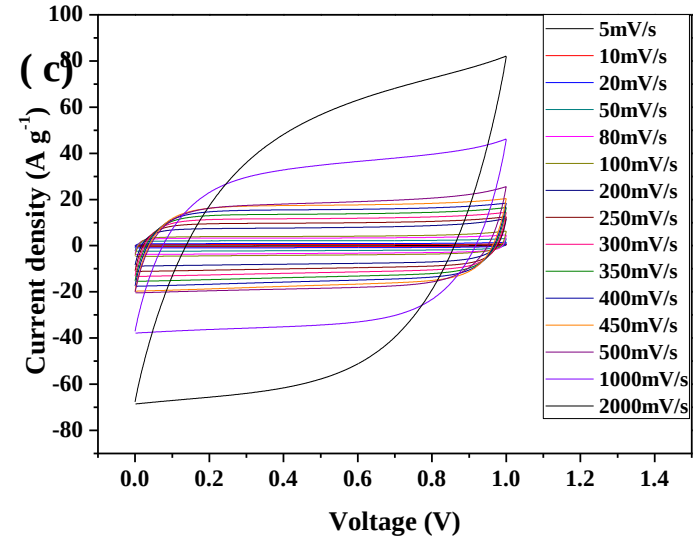
(c)
Current density (A g-1)
Voltage (V)
5mV/s
10mV/s
20mV/s
50mV/s
80mV/s
100mV/s
200mV/s
250mV/s
300mV/s
350mV/s
400mV/s
450mV/s
500mV/s
1000mV/s
2000mV/s

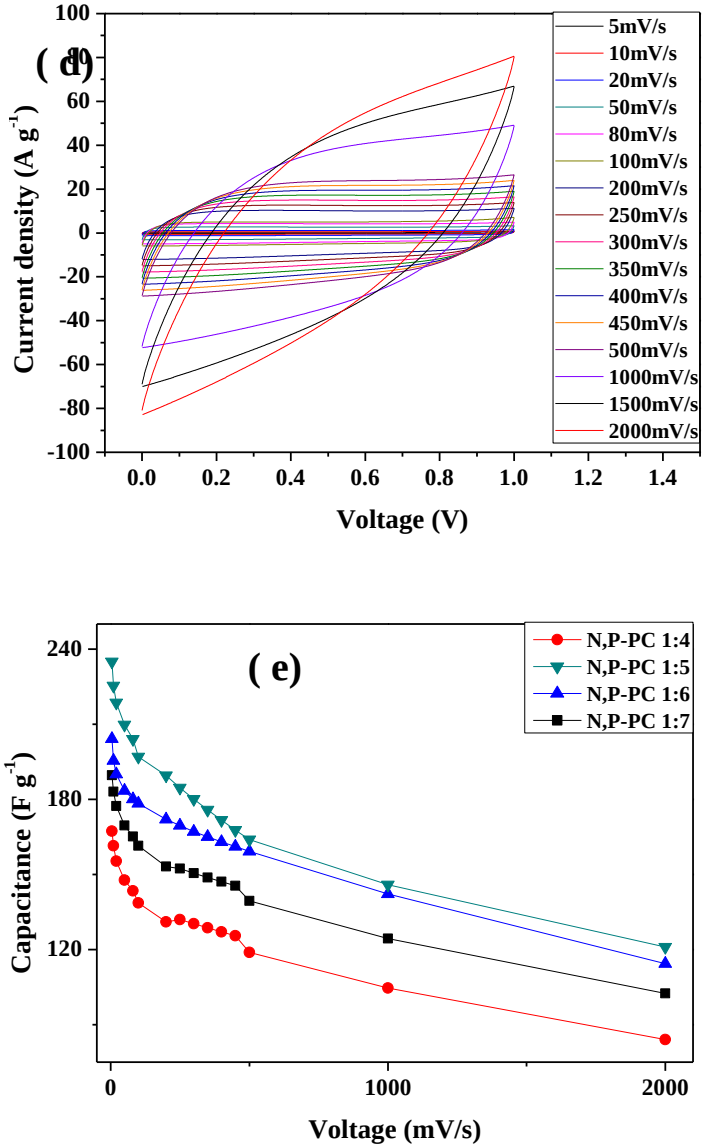

Figure 4. CV curves of the N/P-PC-1:4 (a), N/P-PC-1:5 (b), N/P-PC-1:6 (c), and N/P-PC-1:7 (d) samples at scan rates of 5-2000mV/s. Specific capacitances of the N/P-PC samples at scan rates of 5-2000mV/s (e).

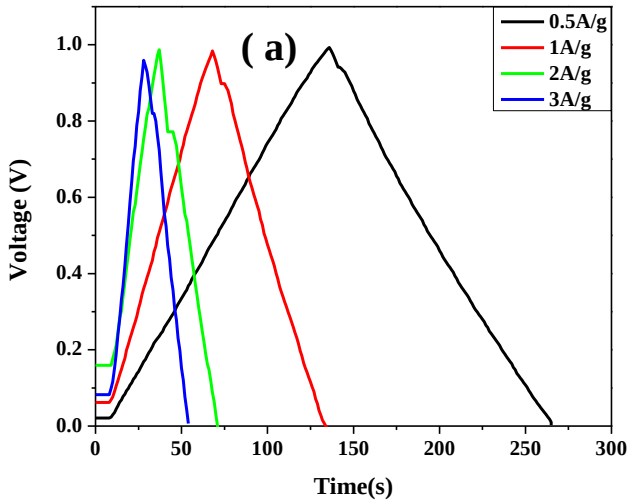

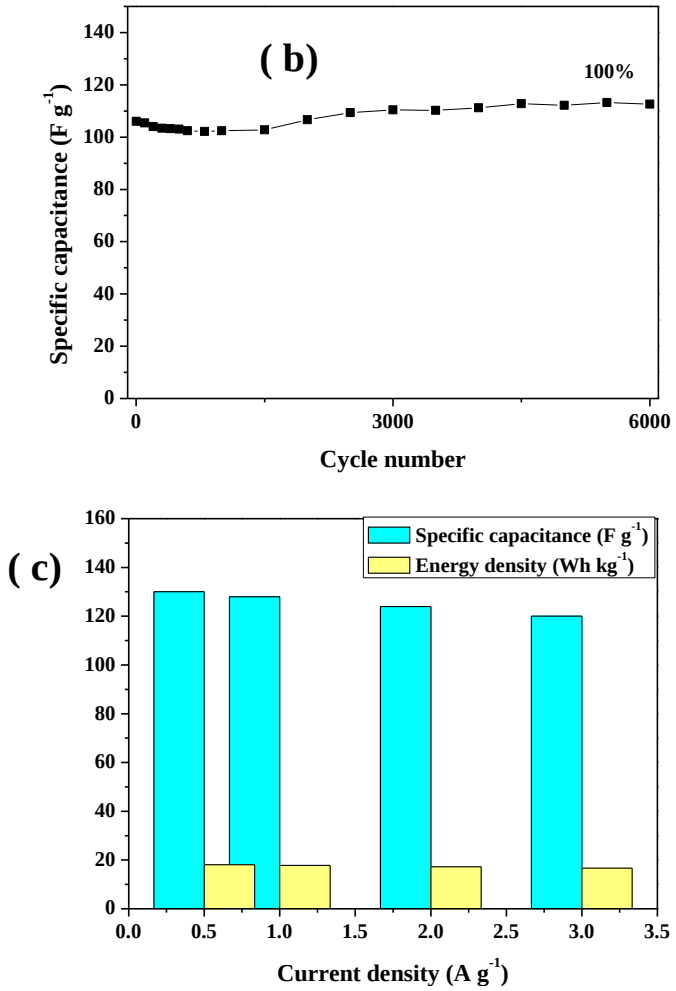

Figure 5. GCD curves of the N/P-PC-1:5 electrode at current densities of 0.5 – 3A/g (a), cycling performance of the N/P-PC-1:5 capacitor at a current density of 10A/g (b), and specific capacitance and energy density of N/P-PC-1:5 at different current densities.

To further probe the supercapacitive properties, the N/P-PC samples were assembled into symmetrical supercapacitors and tested via constant current charge and discharge (GCD) measurements. GCD curves of N/P-PC exhibit quasi-triangular shapes at various current densities and have a very small IR drop (Fig.5a).This indicates typical double-layer capacitive behavior. In addition, the charge of these discharge processes are not completely linear because the doped N and P elements introduce pseudocapacitance. Specific capacitances of the N/P-PC samples in the supercapacitor are calculated using Eq.(2). In Fig.5c, the specific capacitances of the N/P-PC-1:5 electrodes are 130, 127, 124, and 120 F/g at current densities of 0.5, 1, 2, and 3 A/g, respectively. Furthermore, 92.3% capacitance retention is achieved by increasing the current density from 0.5 to 3 A/g, and this indicates the good rate capability of the energy device. In summary, nitrogen and phosphorus doping and hierarchical porous architecture have a significant synergistic effect, enabling the porous carbon materials to have excellent electrochemical performance[32-33]. In addition, the resulting capacitance of the porous carbon samples in an aqueous electrolyte is clearly higher than that of most of the

previously reported materials, which are listed in Table 2.

Table1. Characteristics of N/P-PC prepared with different reaction conditions.

Type of PC	N/P-PC-1:4	N/P-PC -1:5	N/P-PC -1:6	N/P-PC -1:7
Carbonization temperature (°C)	800	800	800	800
Carbonization time (h)	1.0	1.0	1.0	1.0
Impregnation ration	1:4	1:5	1:6	1:7
Yield of activated carbon (wt.%)	40.5%	43.5%	43.0%	44.5%
Typical properties				
BET surface area (m^2/g)	2063	2188	2185	2065
Total pore volume (cm^3/g)	2.978	3.025	3.582	3.86
Average pore diameter (nm)	5.77	5.537	6.946	7.06
Specific capacitance (F/g)	-	130F/g	-	-

Table 2. Comparison of the different biomass precursors of carbon materials for supercapacitor electrodes

Biomass Precursor	Activation method	Electrolyte	S_{BET} (m^2/g)	*Cs* (F/g)	Energy density (Wh/kg)	Ref.
Rice husk	KOH	6M KOH	2696	147	5.11	[13]
Scrap waste tire	H_3PO_4	6M KOH	510	93	-	[14]
Natural wood	KOH	6M KOH	2925	200	-	[15]
Recycled waste paper	KOH	6M KOH	180	180	-	[16]

Rice staw	H_3PO_4	1M H_2SO_4	396	112	-	[17]
Rice husk	H_3PO_4	1M Na_2SO_4	1493	112	15.5	[18]
Wheat straw	$ZnCl_2$ + KCl	6M KOH	1201	223.9	-	[19]
Peaunt shell	KOH	1M H_2SO_4	3616	249	21.53	[20]
Willow catkin	KOH	1M Na_2SO_4	1589	233	21	[21]
Black liquor	KOH	6M KOH	2646	242	9.34	[22]
Rice husk	H_3PO_4	6M KOH	2188	236	17.9	This work

Cycling stability is another key parameter that determines the practical application of supercapacitors. Fig.5b presents specific capacitance versus charge-discharge cycle number for the N/P-PC-1:5 sample at a current density of 10 A/g for 6000 cycle. There is no significant capacitance fading up to cycle 6000, and this suggests the good stability of N/P-PC-1:5. As the results show, the obtained N/P-PC-1:5 porous carbon material has good capacitance behavior and excellent cycling stability, thus, it is a very promising material for supercapacitor electrodes[34].

The energy densities of the N/P-PC-1:5 symmetric supercapacitor were evaluated from the GCD curves using Eq (3). As seen in Fig.5c, the capacitance of the supercapacitor was 130 F/g at a current density of 0.5 A/g, and the energy density was 17.9 Wh/kg. The energy density slightly decreased to 16.85 Wh/kg at a current density of 3 A/g, and these results confirm that doping with an optimal amount of N and P in porous carbon significantly promote the electrochemical performance. In general, the excellent electrochemical properties of carbon materials depend primarily on their hierarchical porous structure and the synergistic effect of nitrogen and phosphorus[44].

4. CONCLUSIONS

In summary, we developed a feasible, low cost, and efficient route for preparing phosphorus and nitrogen co-doped porous carbon from biomass-rice husk as a precursor for carbon. By controlling the amount of the phosphorus source, the obtained N/P-PC materials had unique hierarchical porous carbon structure. It deserves to be mentioned that the N/P-PC-1:5 electrodes show excellent specific capacitance of 130 F/g at a current density of 0.5 A/g and a rate capacitance of 106 F/g at a current density of 10 A/g. The N/P-PC-1:5 electrodes also have a high energy density of 17.9 Wh/kg and long cycle stability. The hierarchical porous structure with nitrogen and phosphorus have a synergistic effect on the excellent performance of the electrochemistry, and this shows that the N/P-PC-1:5 sample with a high content of mesopores is an excellent candidate as an electrode material for supercapacitors. This simple synthesis of co-doped porous carbon can be extended to other biomass material systems to improve the performance of energy storage equipment.

ACKNOWLEDGEMENTS
This research was supported by the National Students' Platform for Innovation and Entrepreneurship Training Program (No. 201510058037), the National Science Foundation of China (51603147 , 11804249, 51908408), and the Science and Technology Correspondent Project of Tianjin (18JCTPJC61300).

References

1. P. Simon, Y. Gogotsi, *Nat. Mater.,* 7 (2008) 845.
2. E. Perricone, M. Chamas, J.C. Leprêtre, P. Judeinstein, P. Azais, E.R. Pinero, F. Béguin, F. Alloin, *J. Power Sources,* 239 (2013) 217.
3. C. Lei, N. Amini, F. Markoulidis, P. Wilson, S. Tennisonb, C. Lekakou, *J. Mater. Chem. A*,1 (2013) 6037.
4. M. Winter, R.J. Brodd, *Chem. Rev.,*35 (2004) 4245.
5. J. Wang, Y.F. Li, L. Yan, Y.N. Qu,*Int. J. Electrochem. Sci.,* 13 (2018) 6259.
6. L.L. Wang, Y.T. Li, K.L. Yang, W.Q. Lu, J.G. Yu, J. Gao, G. Liao, Y.N. Qu, X.F. Wang, X.F. Li, Z. Yin, *Int. J. Electrochem. Sci.*, 12 (2017) 5604.
7. L.L. Zhang, X.S. Zhao,*Chem. Soc. Rev.*, 38 (2009) 2520.
8. P. Simon, Y. Gogotsi, *Nat. Mater.*,7 (2008) 845.
9. C.F. Cheng, S.J. He, C.M. Zhang, C. Du, W. Chen,*Electrochim. Acta*, 290 (2018) 98
10. 10.W.L. Zhang, J.H. Xu, D.X. Hou, J. Yin, D.B. Liu, Y.P. He, H.B. Lin,*Journal of Colloid and Interface Science*, 530 (2018) 338.
11. J. Wang, L.Shen, B.Ding, P.Nie, H.Deng, H.Dou, X.Zhang, *RSC Adv.*, 4(2014)7538.
12. A.G. Pandolfo, A.F. Hollenkamp, *J. Power Sources*,157 (2006) 11.
13. E.Y. Teo, L. Muniandy, E. Ng, F. Adam, A.R. Mohamed, R. Jose, K.F. Chong,*Electrochim. Acta*, 192 (2016) 110.
14. P. Zhao, Y. Han, X. Dong, C. Zhang, S. Liu, *Journal of Solid State Science and Technology*, 4 (2015) 35.
15. L. Chen, T. Ji, L. Brisbin, J. Zhu, *ACS Applied Materials and Interfaces*, 7 (2015) 12230.
16. D. Kalpana, S.H. Cho, S.B. Lee, Y.S. Lee, R. Misra, N.G. Renganathan, *J. Power Sources*, 2 (2009) 587.
17. A. Ganesan, K. Mukerjee, J. Raj, M.M. Shaijumon, *Journal of Porous Material*, 21 (2014) 839.
18. S.G. Lee, K.H. Park, W.G. Shim, M.S. Balathanigaimani, H. Moon, *Journal of Industrial and Engineering Chemistry*, 17 (2011) 450.
19. S.Zhang, K. Tian, B.H. Cheng, H. Jiang, *ACS Sustainable Chem. Eng.*, 5(2017)6682.
20. X.J. Wei, S.G. Wan, X.Q.Jiang, Z. Wang, and S.Y. Gao, *ACS Appl. Mater. Interfaces*, 7(2015)22238.
21. Y.J. Li,G.L.Wang, T. Wei, Z.J. Fan, P. Yan, Nano Energy, 19(2016)165.
22. L.F. Zhu, F. Shen, R. L. Smith Jr, L.L. Yan, L.Y. Li, X.H. Qi, *Chem. Eng. J.*, 316 (2017) 770.
23. L.F. Zhu, F. Shen, R.L. Smith Jr, L.L. Yan, L.Y. Li, X.H. Qi, *Chem. Eng. J.*, 316 (2017) 770.
24. L. Chen, Y.Z. Zuo, Y. Zhang, Y.M. Gao, *Int. J. Electrochem. Sci.*, 13(2018) 642.
25. B.Z. Liu, L.L. Zhang, P.R. Qi, M.Y. Zhu, G. Wang, Y.Q. Ma, *Nanomaterials,* 6 (2016)
26. H.B. Zhao, W.D. Wang, Q.F. Lu, T.T. Lin, Q.L. Lin, H.J. Yang, *Bioresour.Technol.*, 176 (2015) 106.
27. P. Ayala, R. Arenal, M. Rümmeli, A. Rubio, T. Pichler, *Carbon*, 48 (2010)575.
28. T. Durkić, A. Perić, M. Laušević, A. Dekanski, O. Nešković, M. Veljković, Z. Lauševic, *Carbon*, 35 (1997) 1567.
29. H. Konno, T. Ito, M. Ushiro, K. Fushimi, K. Azumi, *J. Power Sources*, 195 (2010)1739.
30. J. Wu, X. Zheng, C. Jin, J. Tian, R. Yang, *Carbon*, 92 (2015) 327.
31. D. Zhang, M. Han, Y. Li, L. Lei, Y. Shang, K. Wang, Y. Wang, Z. Zhang, X. Zhang,H. Feng, *Electrochim. Acta*, 222 (2016)141.

32. L.F. Chen, Z.H. Huang, H.W. Liang, H.L. Gao, S.H. Yu, *Adv. Funct. Mater.*, 24 (2014)5104.
33. W. Yang, W. Yang, A. Song, L. Gao, L. Su, G. Shao, *J. Power Sources*, 359 (2017) 556.
34. C. Wang, L. Sun, Y. Zhou, P. Wan, X. Zhang, J. Qiu, *Carbon*, 59 (2013) 537.
35. X. Yan, Y. Liu, X. Fan, X. Jia, Y. Yu, X. Yang, *J. Power Sources*, 248 (2014) 745.
36. J. Jin, X. Qiao, F. Zhou, Z.S. Wu, L. Cui, H. Fan, *ACS Appl. Mater. Interfaces*, 9 (2017) 17317.
37. Y.N.Qu, Y.M. Tian, B. Zou, J. Zhang, Y.H. Zheng, L.L. Wang, Y. Li, C.G. Rong, Z.C.Wang, *Bioresour. Technol.*, 101(2010) 8402.
38. Y.Q. Zhang, M.M. Jia, H.Y. Gao, J.G. Yu, L.L.Wang, Y.S. Zou, F.M. Qin, Y.N. Zhao, *Electrochim. Acta*, 184 (2015) 32.
39. Y.Q.Zhang, M.M. Jia, J.Q. Yu, J.Q. Fan, L.L. Wang, Y.S. Zou, Y.N. Zhao, *J Solid State Electrochem*, 20(2016)733.
40. M.J. Bleda-Martínez, J.A. Maciá-Agulló, D. Lozano-Castelló, E. Morallón, D. Cazorla-Amorós, A. Linares-Solano, *Carbon*, 43 (2005) 2677.
41. C.L.Wang, Y. Zhou, L. Sun, P. Wan, X. Zhang, J.S. Qiu, *J. Power Sources*, 239 (2013) 81.
42. Y. Zhou, R. Ma, Stephanie L. Candelaria, J.C. Wang, Q. Liu, E. Uchaker, P.X. Li, Y.F. Chen, G.Z. Cao, *J. Power Sources*, 314 (2016) 39.
43. H. Becerril, J.Mao, Z. Liu, R. Stoltenberg, Z. Bao, Y. Chen, *ACS Nano*., 2(2008)463.
44. M. Rosas, J. Bedia, J. Rodriguez-Mirasol, T. Cordero, *Ind. Eng. Chem. Res.*, 47(2008) 1288.